Journal of ELECTRONIC MATERIALS, Vol. 40, No. 5, 2011
DOI: 10.1007/s11664-011-1517-0

An Alternative Approach to Improve the Thermoelectric Properties of Half-Heusler Compounds

BENJAMIN BALKE,[1,2] JOACHIM BARTH,[1] MICHAEL SCHWALL,[1] GERHARD H. FECHER,[1] and CLAUDIA FELSER[1]

1.—Institut für Anorganische Chemie und Analytische Chemie, Johannes Gutenberg-Universität Mainz, 55099 Mainz, Germany. 2.—e-mail: balke@uni-mainz.de

In this report an alternative approach for optimization of the thermoelectric properties of half-Heusler compounds is presented. The common approaches are partial substitution of elements by elements of nearby groups and substitution with homologs. In this approach we substitute one element by one neighboring element with fewer valence electrons and by one with more electrons. The amounts of the substitutions are chosen such that the amount of deficiency and excess electrons are compensated. In the solid solution $TiCo_x(Ni_{0.5}Fe_{0.5})_{1-x}Sb$, Co was substituted equally by Fe and Ni. The aim of the substitution was to improve the figure of merit by a reduction of the thermal conductivity accompanied by an unchanged high Seebeck coefficient. The solid solution $TiCo_x(Ni_{0.5}Fe_{0.5})_{1-x}Sb$ was synthesized by arc-melting. The structure of the as-cast samples was analyzed by x-ray diffraction. Rietveld refinements yielded the $C1_b$ structure type with a small amount of antisite disorder between Co and Sb. The thermoelectric properties of the solid solution were investigated in the temperature range from 2 K to 400 K. A Seebeck coefficient of $-260\,\mu V\,K^{-1}$ at 400 K and a reduction of the thermal conductivity to $3\,Wm^{-1}\,K^{-1}$ were measured. The figure of merit was enhanced by a factor of about seven to a value of 0.04 at 400 K for $TiCo_{0.8}(Ni_{0.1}Fe_{0.1})Sb$.

Key words: Heusler compounds, thermal conductivity, thermoelectrics

INTRODUCTION

Thermoelectric (TE) materials and their use as energy converters have been intensively discussed lately.[1–5] Decisive for the conversion efficiency is the figure of merit (ZT), which is defined by

$$ZT = \frac{S^2}{\rho\kappa}T, \tag{1}$$

where S, ρ, κ, and T are the Seebeck coefficient, electrical resistivity, thermal conductivity, and absolute temperature, respectively. The threshold for economical use, besides other conditions, is a ZT value larger than 1. A very promising material class in this field are the Heusler XYZ compounds that crystallize in the AlLiSi structure type. High ZT values of up to 1.4 have been obtained in several compounds that exhibit this structure type.[5,6] A compound of this material class is TiCoSb.[7–12]

Calculations predict an energy gap of 0.95 eV[13,14] at the Fermi energy, which indicates the maximum figure of merit to be in the high temperature range. The optimum band gap E_{Gap} of a thermoelectric material and its resulting optimized operating temperature T can be estimated by

$$E_{Gap} = nk_BT, \tag{2}$$

with n between 6 and 10, where k_B is the Boltzmann constant.[15–17] n depends strongly on the scattering mechanism, and whether it is of parabolic or nonparabolic nature. The resulting optimized operating temperature is between 1103 K and 1838 K for TiCoSb. Therefore, TiCoSb is supposed to be a

(Received May 7, 2010; accepted January 7, 2011; published online March 24, 2011)

suitable material for a high-temperature application. However, it has to be taken into account that disorder reduces the gap and consequentially the optimized operating temperature. A high operating temperature is desirable because there exist many such applications where waste heat could be recovered using TE generators. A precondition for high working temperature is chemical stability. A major aspect influencing the chemical stability is the homogeneous and stoichiometric composition of a compound. Synthesis of stoichiometric and homogeneous TiCoSb is challenging, due to evaporation of Sb during synthesis.[18,19] Small amounts of disorder and nonstoichiometric amounts of Sb change the electronic band structure significantly.[20] Loss of Sb during arc-melting cannot be monitored by standard x-ray diffraction (XRD) because it is below its detection range. It has been shown that annealing does not improve the thermoelectric properties for TiCoSb-based compounds.[18] Loss of Sb during synthesis causes several problems, e.g., fast degradation during use, hard reproducibility, and automatic doping, so great care has to be taken during synthesis to ensure reproducible results. In this report an alternative approach for optimization of the thermoelectric properties of Heusler compounds is presented. The common approaches are partial substitution of elements by elements of nearby groups and substitution with homologous elements. In our new approach we substitute one neighboring element with fewer valence electrons and one with more electrons. The amounts of the substitutions are chosen such that the amounts of deficiency and excess electrons are compensated. Therefore, the amount of valence electrons is not changed and the semiconducting properties should be maintained.[21] The compound $TiNi_{0.5}Fe_{0.5}Sb$ is well known and characterized.[22] Here, the solid solution $TiCo_x(Ni_{0.5}Fe_{0.5})_{1-x}Sb (0 \leq x \leq 1)$ was synthesized, and the thermoelectric properties were investigated.

EXPERIMENTAL PROCEDURES

The solid solution $TiCo_x(Fe_{0.5}Ni_{0.5})_{1-x}Sb$ was prepared by arc-melting of stoichiometric amounts of the elements. The composition was $TiCo_x(Ni_{0.5}Fe_{0.5})_{1-x}Sb$ ($x = 0, 0.4, 0.6, 0.8, 1$). Special care was taken to avoid oxygen contamination. This was ensured by melting Ti inside the vacuum chamber before melting the compound. To ensure the homogeneity of the samples, they were remelted several times and flipped before each melting step. Each sample was weighed after each melting step. The samples were not annealed due to the known loss of Sb and the decrease of homogeneity during the annealing step.[18] This procedure resulted in samples exhibiting the $C1_b$ structure. Bars of about 2 mm × 2 mm × 8 mm were cut from the pellets and polished before measuring.

For powder investigations, the remainder was crushed by hand using a mortar. The structure has been investigated by x-ray powder diffraction using Mo K_α radiation (Bruker D8 Advance).

Measurements of the Seebeck coefficient, thermal conductivity, and electric resistivity were carried out using a physical property measurement system (PPMS) model 6000 (Quantum Design) equipped with the options P400, P600, and P640. The bars were contacted by copper stripes that were wrapped around the sample to homogenize the current. Additionally, the stripes were glued to the sample with a silver epoxy paste to improve the contact. Before contacting, the samples were polished to remove oxide layers which may have formed in the time between synthesis and measurement. The thermoelectric properties were measured at pressure of about 1.2×10^{-4} mbar. An additional correction term for heat loss at the heating shoes was introduced and applied to the thermal conductivity data, as suggested by Müller et al.[23] and Quantum Design.[24] Due to known problems of the PPMS with the evaluation of thermal conductivity data above 250 K, a correction factor was introduced. For the samples the empirical equation

$$\kappa_{cor} = \kappa_{exp} - AT^3 \quad (3)$$

was used. κ_{cor} is the corrected value of the thermal conductivity, κ_{exp} is the measured value of the thermal conductivity, and A is an empirically determined parameter that depends on the length of the wires and their cross-section, as well as the length and cross-section of the sample.

RESULTS AND DISCUSSION

Structural Properties

X-ray diffraction was performed on the compounds. As an example the XRD pattern for $TiCo_{0.8}Ni_{0.1}Fe_{0.1}Sb$ is shown in Fig. 1. The relatively sharp reflections highlight the good crystallinity of all the samples. Rietveld refinement was performed on the pattern, assuming space group $F\bar{4}3m$ with Ti at the 4a Wyckoff position, Sb at the 4b position, Co, Ni, and Fe at the 4c position, and an assumed empty 4d position, as should be the case for a well-ordered $C1_b$ structure. The refinement yielded the best pattern R-factors for an assumed antisite disorder of 5% between the Sb at the 4b position and the Co at the 4c position. Additional occupation of the 4d sublattice by excess Sb increased the R value of the refinement with increasing occupation of the 4d position. Therefore, it is assumed that the 4d sublattice is vacant and not filled with excess Sb. All samples showed the $C1_b$ structure. A refinement of the powder pattern for TiCoSb yielded a lattice parameter of 5.879 Å. This is in agreement with the values found in the literature of 5.884 Å[25] and 5.979 Å.[26] The change of the lattice parameter by the substitution is displayed in the inset of Fig. 1. A linear fit was applied to prove whether $a(x)$ follows Vegard's law.[27] The equation resulting from the

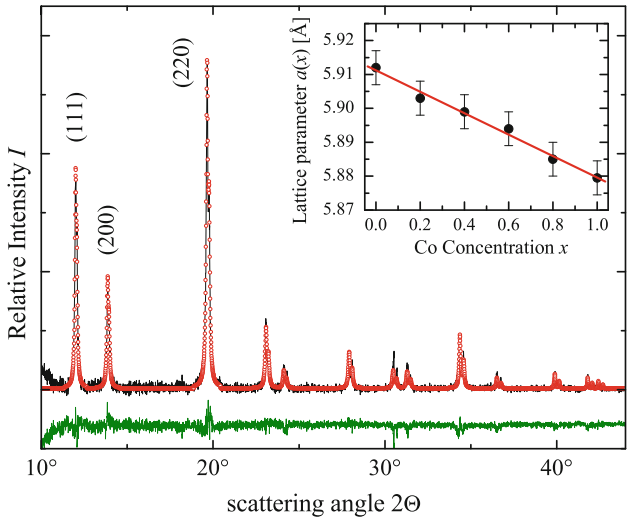

Fig. 1. XRD pattern of $TiCo_{0.8}Ni_{0.1}Fe_{0.1}Sb$. In the inset the lattice parameters for $TiCo_x(Ni_{0.5}Fe_{0.5})_{1-x}Sb$ are displayed. The line is a result of a linear curve fit.

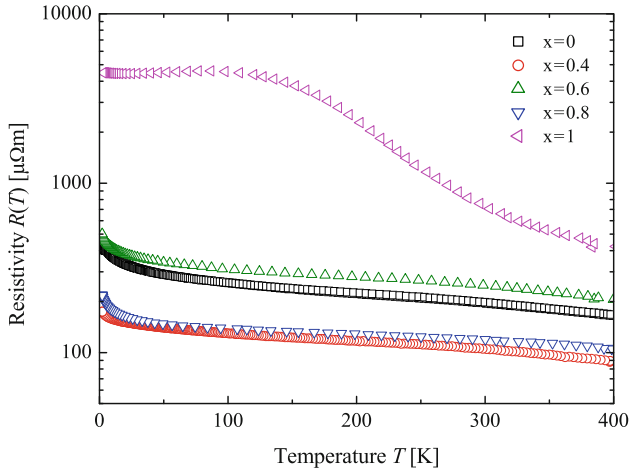

Fig. 2. Electric resistivity data for $TiCo_x(Ni_{0.5}Fe_{0.5})_{1-x}Sb$.

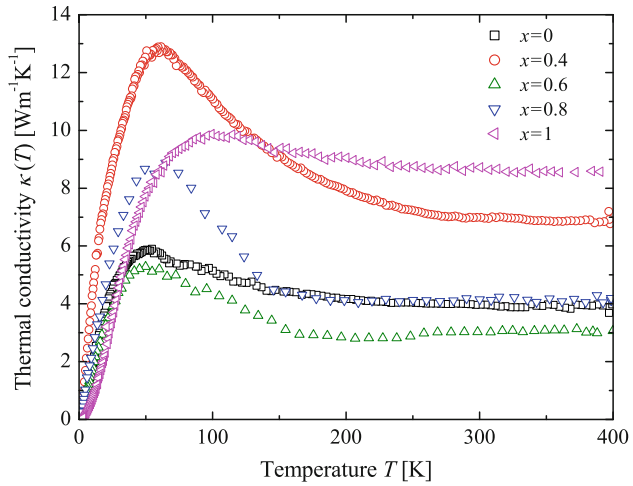

Fig. 3. Thermal conductivity data for $TiCo_x(Ni_{0.5}Fe_{0.5})_{1-x}Sb$.

linear fit is $a(x) = -0.032x + 5.911$ Å. It should be noted that, with decreasing Co content, the lattice parameter increased. The average size of Ni and Fe are not equal to that of Co in this solid solution. In all samples—except the pure TiCoSb—small amounts (less than 1%) of kamacite (Ni;Fe) impurities were observed. These small metallic inclusions were randomly distributed throughout the whole sample with a size of approximately 10 μm. How this impurity and the above-mentioned disorder in the samples could influence the different transport properties is discussed in the corresponding sections below.

Transport Properties

Electrical Resistivity

The resistivity was measured in the range from 2 K to 400 K. The determined resistivity values of the first and the last element of the solid solution $x = 0$ and $x = 1$, $TiNi_{0.5}Fe_{0.5}Sb$[22] and TiCoSb,[28,29] agree well with the findings reported in the literature. For both TiCoSb and $TiNi_{0.5}Fe_{0.5}Sb$, typical semiconducting behavior is observed. According to Ref. 21 both $C1_b$ compounds should be semiconducting, because they possess 18 valence electrons. The calculated band gaps are 0.95 eV[13] and 0.8 eV[22] for TiCoSb and $TiNi_{0.5}Fe_{0.5}Sb$, respectively. Therefore, it is assumed that the band gap decreases with lower Co concentrations. This explains the principle trend of the decrease of the resistivity with decreasing x in $TiCo_x(Ni_{0.5}Fe_{0.5})_{1-x}Sb$ (Fig. 2). A perfect fit of the values for the intermediate compounds ($x = 0.4, x = 0.6$, and $x = 0.8$) could not be observed due to the strong influence on the resistivity for small amounts of disorder and impurities.

Thermal Conductivity

Figure 3 shows the measurement results of the thermal conductivity of all the compounds. The thermal conductivity was measured in the temperature range from 2 K to 400 K. For the Co concentrations $x = 0.8$, $x = 0.6$, and $x = 0$, the lowest overall thermal conductivities were determined. The lowest observed values are about 3 $Wm^{-1}K^{-1}$ at 300 K, which is among the lowest known values for $C1_b$ compounds. A decrease in the thermal conductivity has been achieved. This decrease cannot be explained by mass fluctuation scattering only, since the mass differences of Fe, Co, and Ni are small. The reduction of the thermal conductivity from TiCoSb to $TiCo_{0.6}Ni_{0.2}Fe_{0.2}Sb$ is about 60%. A reduction of the thermal conductivity by the substitution of Fe for Co was reported before by Wu et al.[7] It can be estimated by the Wiedemann–Franz law that the thermal conductivity is dominated by the lattice thermal conductivity.[30] The reduction is supposed

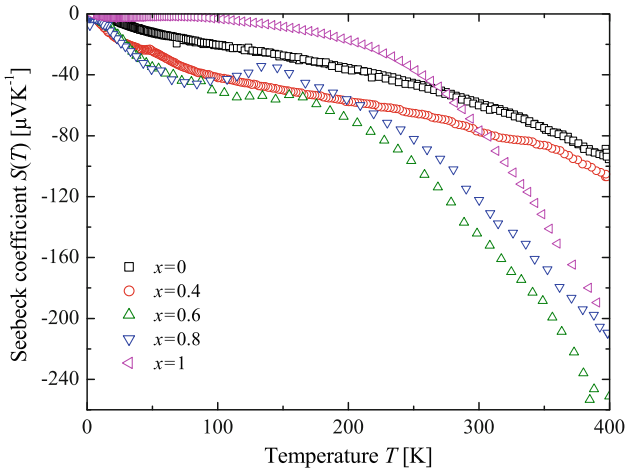

Fig. 4. Seebeck coefficient data for $TiCo_x(Ni_{0.5}Fe_{0.5})_{1-x}Sb$.

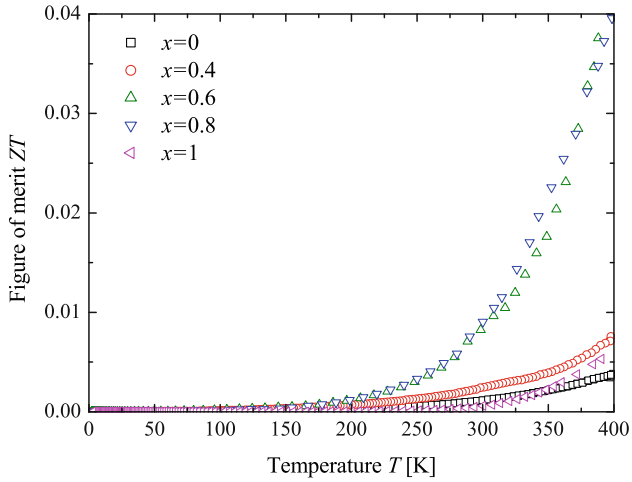

Fig. 5. Figure of merit for $TiCo_x(Ni_{0.5}Fe_{0.5})_{1-x}Sb$.

to consist of several effects, which are magnetic scattering of phonons by Fe ions, a small amount of additional impurities, and mass fluctuation. The pronounced maxima of the thermal conductivity at lower temperatures is typical for crystals with many atoms in the unit cell.[31]

Seebeck Coefficient

In Fig. 4 the measurements of the Seebeck coefficient in the temperature range from 2 K to 400 K are shown. The values for TiCoSb agree well with the findings of Zhou et al.[8] For $TiNi_{0.5}Fe_{0.5}Sb$, a value of $-60\,\mu V\,K^{-1}$ at 300 K was obtained. The Seebeck coefficient for $TiNi_{1-x}Fe_xSb$ is very sensitive to the amount of Fe and Ni.[22] For the Co concentrations of $x = 0$ and $x = 0.4$ the Seebeck coefficient is not significantly influenced. For $TiCo_{0.8}Ni_{0.1}Fe_{0.1}Sb$ and $TiCo_{0.6}Ni_{0.2}Fe_{0.2}Sb$ an increase of the Seebeck coefficient is observed. The raised absolute values of S for $TiCo_{0.6}Ni_{0.2}Fe_{0.2}Sb$, $TiCo_{0.8}Ni_{0.1}Fe_{0.1}Sb$, and $TiCo_{0.4}Ni_{0.3}Fe_{0.3}Sb$ at low temperatures are probably related to a phonon drag effect.[32] An additional indication for this effect is the pronounced peak of the thermal conductivity in this temperature range for these compounds. The highest achieved Seebeck coefficient increase of about 35% at 400 K was found for $TiCo_{0.6}Ni_{0.2}Fe_{0.2}Sb$ compared with TiCoSb. The negative sign of the Seebeck coefficient indicates that the electric conductivity is dominated by electrons.

The figure of merit of the compounds was calculated from the measured values in the temperature range from 2 K to 400 K. The results are displayed in Fig. 5. The largest improvement compared with TiCoSb was achieved with the compounds $TiCo_{0.6}Ni_{0.2}Fe_{0.2}Sb$ and $TiCo_{0.8}Ni_{0.1}Fe_{0.1}Sb$. The improvement is mainly based on the reduction of the thermal conductivity and the electrical resistivity.

CONCLUSIONS

In this report an alternative approach for optimization of the thermoelectric properties of half-Heusler compounds is presented. The approach is based on the substitution of one element by one neighboring element with fewer valence electrons and one with more electrons. The amounts of the substitutions are chosen such that the amount of deficiency and excess valence electrons are compensated. As an example, Co was substituted in equal parts by Ni and Fe in the solid solution $TiCo_x(Ni_{0.5}Fe_{0.5})_{1-x}Sb$. Substitution of Co by Ni and Fe is an efficient approach to improve the figure of merit. The enhancement is based on the reduction of the thermal conductivity and an accompanying increase of the Seebeck coefficient. The small amounts (less than 1%) of metallic kamacite (Ni;Fe) impurities in the samples can cause a decrease in the electric resistivity and the Seebeck coefficient accompanied by an increase of the thermal conductivity. The slight antisite disorder (5%) can cause a reduction of the thermal conductivity and the electric conductivity. However, since these effects are existent in all samples, the observed influence of the Ni and Fe substitution on the transport properties are unambiguously distinguishable. The reduction of the thermal conductivity is probably caused by several effects, which are magnetic scattering of phonons by Fe ions and mass fluctuations. In combination with other reported improvements for TiCoSb, the reported results should lead to respectable ZT values. Further enhancements can be achieved by partial substitution of other constituents in the compound, as suggested by several other studies.[7–12]

ACKNOWLEDGEMENTS

The authors appreciate the financial support of the project through the Stiftung Rheinland-Pfalz für Innovation (Project 863).

REFERENCES

1. D. Rowe, *CRC Handbook of Thermoelectrics* (Boca Raton, FL: CRC, 1995).
2. H.J. Goldsmid, *CRC Handbook of Thermoelectrics* (Boca Raton, FL: CRC, 1995).
3. B. Sales, B. Chakoumakos, D. Mandrus, and J. Sharp, *J. Solid State Chem.* **146**, 528 (1999).
4. B. Sales, D. Mandrus, B.C. Chakoumakos, V. Keppens, and J. Thompson, *Phys. Rev. B* **56**, 15081 (1997).
5. S. Sakurada and S. Shutoh, *Appl. Phys. Lett.* **86**, 2105 (2005).
6. Y. Kimura, T. Kuji, A. Zama, Y. Shibata, and Y. Mishima, *Solid-State Ionics* (2006).
7. T. Wu, W. Jian, X. Li, Y. Zhou, and L. Chen, *J. Appl. Phys.* **102**, 1037051 (2007).
8. M. Zhou, L. Chen, C. Feng, D. Wang, and J. Li, *J. Appl. Phys.* **101**, 1137141 (2007).
9. K. Kroth, B. Balke, G. Fecher, V. Ksenofontov, C. Felser, and H.J. Lin, *Appl. Phys. Lett.* **89**, 202509 (2006).
10. V. Ksenofontov, K. Kroth, S. Reiman, F. Casper, V. Jung, M. Takahashi, M. Takeda, and C. Felser, *Hyp. Int.* **168**, 1201 (2006).
11. W. Ting, W. Jiang, X. Lia, S. Baia, S. Liufu, and L. Chen, *J. Alloys Compd.* **467**, 590 (2009).
12. L.L. Wang, L. Miao, Z.Y. Wang, W. Wei, R. Xiong, H.J. Liu, J. Shi, and X.F. Tang, *J. Appl. Phys.* **105**, 013709 (2009).
13. J. Tobola, J. Pierre, S. Kaprzyk, R.V. Skolozdra, and M.A. Kouacou, *J. Phys.: Condens. Matter.* **10**, 1013 (1998).
14. B. Balke, G.H. Fecher, A. Gloskovskii, J. Barth, K. Kroth, F. Felser, R. Robert, and A. Weidenkaff, *Phys. Rev. B* **77**, 045209 (2008).
15. J.O. Sofo and G.D. Mahan, *Phys. Rev. B* **49**, 4565 (1994).
16. R. Chasmar and R. Stratton, *J. Electron. Control* **7**, 52 (1959).
17. G.D. Mahan, *J. Appl. Phys.* **65**, 1578 (1989).
18. T. Sekimoto, K. Kurosaki, H. Muta, and S. Yamanaka, *J. Alloys Compd.* **394**, 122 (2005).
19. Y. Stadnyka, V.A. Romaka, M. Shelyapina, Y. Gorelenko, L. Romaka, D. Fruchart, A. Tkachuk, and V. Chekurin, *J. Alloys Compd.* **421**, 19 (2006).
20. B. Balke, K. Kroth, G. Fecher, and C. Felser, *J. Appl. Phys.* **103**, 07D115 (2008).
21. D. Jung, H.J. Koo, and M.H. Whangbo, *J. Mol. Struc. (THEOCHEM)* **527**, 113 (2000).
22. J. Tobola, L. Jodin, P. Pecheur, H. Scherrer, G. Venturini, B. Malaman, and S. Kaprzyk, *Phys. Rev. B.* **64**, 155103 (2001).
23. E. Müller, C. Stiewe, D. Rowe, and S. Williams, *Thermoelectrics Handbook Macro To Nano* (Boca Raton: CRC, 2006).
24. Q. Design, *Physical Property Measurement System Thermal Transport Option User's Manual* (USA, San Diego: Quantum Design, 2002).
25. P.J. Webster and K. Ziebeck, *J. Phys. Chem. Solids* **34**, 1647.
26. A. Szytula, Z. Tomkowicz, and M. Turowski, *Acta Phys. Pol. A* **44**, 147 (1973).
27. L. Vegard, *Zeitschr. f. Phys. A Hadr. Nucl.* **5**, 17 (1921).
28. N. Tareuchi, K. Gosho, M. Hiroi, and M. Kawakami, *Phys. B: Condens. Mater.* **359–361**, 1183 (2005).
29. Y. Xia, V. Ponnambalam, S. Bhattacharya, A.L. Pope, S.J. Poon, and T.M. Tritt. *J. Phys.: Condens. Mater.* **13**, 7789 (2001).
30. C. Bhandari and R. Rowe, *Thermal Conduction in Semiconductors* (New Delhi, India: Wiley Eastern, 1988).
31. V. Zaitsev and M. Fedorov, *Thermoelectrics Handbook Macro To Nano* (Boca Raton: CRC, 2006).
32. C.M. Bhandari, *CRC Handbook of Thermoelectrics* (Boca Raton: CRC, 1995).